HHS Public Access

Author manuscript

Oncogene. Author manuscript; available in PMC 2014 August 27.

Published in final edited form as:

Oncogene. 2014 February 27; 33(9): 1101–1112. doi:10.1038/onc.2013.69.

15-PGDH inhibits hepatocellular carcinoma growth through 15-keto-PGE_2/PPARγ-mediated activation of $p21^{WAF1/Cip1}$

Dongdong Lu[1,2], **Chang Han**[1], and **Tong Wu**[1]

[1]Department of Pathology and Laboratory Medicine, Tulane University School of Medicine, New Orleans, LA

[2]Tongji University School of Life Science and Technology, Shanghai, China

Abstract

15-hydroxyprostaglandin dehydrogenase (15-PGDH) is a key enzyme in prostaglandin metabolism. This study provides important evidence for inhibition of hepatocellular carcinoma (HCC) growth by 15-PGDH through the 15-keto-PGE_2/PPARγ/$p21^{WAF1/Cip1}$ signaling pathway. Forced overexpression of 15-PGDH inhibited HCC cell growth *in vitro*, whereas knockdown of 15-PGDH enhanced tumor growth parameters. In a tumor xenograft model in SCID mice, inoculation of human HCC cells (Huh7) with overexpression of 15-PGDH led to significant inhibition of tumor growth, while knockdown of 15-PGDH enhanced tumor growth. In a separate tumor xenograft model in which mouse HCC cells (Hepa1-6) were inoculated into syngeneic C57BL/6 mice, intratumoral injection of adenovirus vector expressing 15-PGDH (pAd-15-PGDH) significantly inhibited xenograft tumor growth. The anti-tumor effect of 15-PGDH is mediated through its enzymatic product, 15-keto-PGE_2, which serves as an endogenous PPARγ ligand. Activation of PPARγ by 15-PGDH-derived 15-keto-PGE_2 enhanced the association of PPARγ with the $p21^{WAF1/Cip1}$ promoter and increased p21 expression and association with CDK2, CDK4 and PCNA. Depletion of p21 by shRNA reversed 15-PGDH-induced inhibition of HCC cell growth; overexpression of p21 prevented 15-PGDH knockdown-induced tumor cell growth. These results demonstrate a key 15-PGDH/15-keto-PGE_2-mediated activation of PPARγ and $p21^{WAF1/Cip1}$ signaling cascade that regulates hepatocarcinogenesis and tumor progression.

Keywords

Hepatocellular carcinoma (HCC); 15-hydroxyprostaglandin dehydrogenase (15-PGDH); 15-keto-PGE_2; p21; PPARγ; liver

Address correspondence to: Tong Wu, M.D., Ph.D., Department of Pathology and Laboratory Medicine, Tulane University School of Medicine, 1430 Tulane Avenue, SL-79, New Orleans, LA 70112. Tel: 504-988-5210, Fax: 504-988-7862, twu@tulane.edu.

The authors declare no conflict of interest.

INTRODUCTION

Hepatocellular carcinoma (HCC) is a primary malignancy of the liver and its incidence is rising in the United States and around the world(1–4). The tumorigenic process is characterized by dysregulation of cell cycle progression and abnormal cell proliferation in the setting of chronic inflammation and fibrosis of the liver parenchyma. Consistent with the strong association between chronic inflammation and hepatocarcinogenesis, studies have shown that mediators of inflammation, such as prostaglandins (PGs), play an important role in hepatocarcinogenesis(5–7). Previous studies have been focused on defining the role of cyclooxygenase-2 (COX-2, a key enzyme that mediates prostaglandin synthesis) in HCC. Indeed, the expression of COX-2 is increased in human and animal HCCs and in dysplastic hepatocytes(5–7). In cultured HCC cells, forced overexpression of COX-2 increases tumor cell growth and invasiveness. Selective and non-selective COX-2 inhibitors prevent HCC cell growth *in vitro* and in animal models of hepatocarcinogenesis(5–7), although these inhibitors are known to mediate effects through both COX-dependent and -independent mechanisms. These findings suggest the possibility of targeting COX-2 for prevention and treatment of HCC in patients. This approach is expected to be safe, given that selective COX-2 inhibitors do not adversely affect renal function in cirrhosis(8, 9) (in contrast to NSAID-related renal failure in decompensated cirrhosis). However, on the other hand, in light of the increased cardiovascular side effect associated with some COX-2 inhibitors(10–13), it is imperative to identify specific molecular targets downstream of COX-2 for effective and safer anti-HCC therapy.

The amount of biologically active PGE_2 is regulated by the balance of PGE_2 synthesis and degradation. The NAD+-linked 15-hydroxyprostaglandin dehydrogenase (15–PGDH) is a member of the short-chain nonmetalloenzyme alcohol dehydrogenase protein family, which catalyzes oxidation of the 15(S)-hydroxyl group of PGE_2, converting PGE_2 into 15-keto-PGE_2(14). This enzymatic reaction causes inactivation of PGE_2, a pro-inflammatory and pro-tumorigenic lipid mediator. Several recent studies suggest a tumor suppressive role of 15-PGDH in several non-hepatic cancers(15–23). However, to date, the action of 15-PGDH is largely attributable to its degradation of biologically active PGE_2, with its 15-keto metabolite being considered largely inactive, and it remains unknown whether 15-PGDH is implicated in hepatocellular carcinoma.

This study was designed to examine the biological function and molecular mechanism of 15-PGDH in hepatocellular carcinoma by using complementary *in vitro* and *in vivo* approaches. We show herein that the anti-tumor effect of 15-PGDH is mediated through its enzymatic product, 15-keto-PGE_2, which activates peroxisome proliferator-activated receptor γ (PPARγ) leading to $p21^{WAF1/Cip1}$ expression and association with key downstream molecules including CDKs and PCNA. Our data shift the current paradigm and disclose an important 15-PGDH/15-keto-PGE_2-mediated activation of PPARγ and $p21^{WAF1/Cip1}$ signaling axis that suppresses hepatocarcinogenesis and tumor progression.

RESULTS

15-PGDH inhibits HCC cell growth *in vitro*

To determine the role of 15-PGDH in HCC cell growth, we established human HCC cells with stable overexpression or knockdown of 15-PHDH. Human HCC cell line (Huh7) was stably transfected with the GFP control vector (pCMV6-AC-GFP), 15-PGDH expression vector (pCMV6-AV-GFP-15PGDH), RNAi control vector (pGFP-V-RS), and 15-PGDH RNAi vector (pGFP-V-RS-15PGDH), respectively; successful overexpression or knockdown of 15-PGDH was confirmed by immunofluorescence and western blotting (Figure 1A). Under immunofluorescence, the intensity of 15-PGDH staining was higher in 15-PGDH overexpressed cells and decreased in 15-PGDH knockdown cells. Under western blotting analysis, the level of 15-PGDH protein was increased in Huh7 cells transfected with the 15-PGDH overexpression vector (56KD GFP-15PGDH fusion protein) and decreased in cells transfected with the 15-PGDH RNAi vector (29KD monomeric form, 58KD dimeric form). The aforementioned stable cell lines were cultured *in vitro* and their growth curves over time were measured by WST-1 assay. As shown in Figure 1B, overexpression of 15-PGDH inhibited cell growth, whereas RNAi knockdown of 15-PGDH enhanced it. Flow cytometry analysis showed that 15-PGDH overexpression increased the cells in G0/G1 phase (65.2±10.2% versus 42.1±9.7%, $p < 0.05$) and decreased the cells in S phase (22.7±4.2% versus 47.3%±9.8, $p < 0.01$) (Figure 1C). In contrast, 15-PGDH knockdown decreased the cells in G0/G1 phase (20.2% versus 45.2 %, $p < 0.01$) and increased the cells in S phase (69.4 ±11.8% versus 45.1±10.9%, $p < 0.05$). The percentages of cells in G2 phase were not significantly altered when 15-PGDH was overexpressed or knocked down. Immunofluorescence for BrdU (a S phase marker) showed that the BrdU positive cells were lower in 15-PGDH overexpressed cells (6.71±1.52% compared to 39.41±8.13% in the corresponding control) and higher in 15-PGDH knockdown cells (81.84±13.24% compared to 35.52±5.78% in the corresponding control) (Figure 1D). Soft agar clonogenic assay showed that overexpression of 15-PGDH reduced clonogenic growth, whereas knockdown of 15-PGDH enhanced it. The colony formation rates for the two mock Huh7 cells lines were 23.4±4.5% and 24.5±6.2%, respectively, while the colony formation rate was 5.67±1.59% for 15-PGDH overexpressed cells and 61.4±11.87% for 15-PGDH knockdown cells (Figure 1E). Taken together, these findings demonstrate that 15-PGDH signaling induces HCC cell cycle arrest at G1/S transit and inhibits cell proliferation, DNA synthesis and clonogenic growth.

15-PGDH inhibits HCC growth in SCID mice

To examine the effect of 15-PGDH signaling on HCC growth *in vivo*, the above four stable Huh7 cell lines were inoculated into SCID mice and the animals were closely monitored for tumor development. As shown in Figure 2A, 15-PGDH overexpression inhibited tumor growth whereas 15-PGDH depletion accelerated growth. When 15-PGDH was overexpressed, the tumor weight decreased to approximately one-third of the control group (0.208±0.057g versus 0.748±0.153g, $p < 0.01$). Conversely, when 15-PGDH was knocked down, the tumor weight increased approximately three fold compared to the control group (2.311±0.498g versus 0.681±0.124g, $p < 0.01$). The tumor appearance time in 15-PGDH overexpressed group was prolonged (15.13±4.27 days versus 8.12±3.24 days in the control

group, $p < 0.01$); in contrast the tumor appearance time in 15-PGDH knockdown group was shortened (5.98±2.13 days versus 9.03±3.19 days in the control group, $p < 0.01$). Immunohistochemical staining for the proliferating cell nuclear antigen (PCNA) showed that the percentage of PCNA-positive cells was significantly lower in 15-PGDH overexpressed tumors (18.24±2.99%) compared to the control group (36.83±9.51%, $p < 0.01$). In contrast, the percentage of PCNA-positive cells was significant higher in 15-PGDH knockdown tumors (91.22±11.86%) compared to the control group (41.32±6.31%, $p < 0.01$) (Figure 2B). Accordingly, western blotting confirmed that the level of PCNA was lower in 15-PGDH overexpressed tumors and higher in 15-PGDH knockdown tumors (Figure 2C). Furthermore, 15-PGDH overexpression increased the expression level of the cyclin kinase inhibitor $p21^{WAF1/Cip1}$ in xenograft tumors, whereas 15-PGDH knockdown reduced it (Figure 2C).

15-PGDH inhibits HCC growth in C57BL/6 mice

We next utilized a complementary syngeneic HCC xenograft model in which a murine HCC cell line originated from C57BL/6 mouse strain (Hepa1-6) was inoculated subcutaneously at armpit in C57BL/6J mice. When the tumors become palpable, an adenoviral vector expressing 15-PGDH (pAd-15-PGDH) or the pAd control vector was directly injected into the tumor modules (at three day interval, starting 10 days after inoculation till the end of the experiment). The tumor size in the pAd-15-PGDH injected group was significantly smaller compared to the pAd-control group ($p < 0.01$) (Figure 3A). The average tumor weight in pAd-15-PGDH treated group was also significantly lower compared to the pAd control group (0.57±0.12 grams versus 2.51±0.58 grams $p < 0.01$) (Figure 3B). Increased 15-PGDH protein in pAd-15PGDH treated tumors was confirmed by Western blotting analysis (Figure 3C). pAd-15PGDH treatment decreased PCNA expression in xenograft tumor cells (Figure 3D-E). Furthermore, treatment with pAd-15PGDH increased the level of $p21^{WAF1/Cip1}$ (predominantly in the nuclei) (Figure 3E-F). These findings further demonstrate that 15-PGDH inhibits the progression of HCC *in vivo* and suggest that a potential role of $p21^{WAF1/Cip1}$.

15-PGDH-derived 15-keto-PGE_2 activates PPARγ in HCC cells

We observed an inverse alteration of PGE_2 and 15-keto-PGE_2 metabolite levels in cells with altered 15-PGDH expression. As shown in Figure 4A and 4B, 15-PGDH overexpressed cells exhibited decreased PGE_2 and increased 15-keto-PGE_2 metabolite, whereas 15-PGDH knockdown cells had increased PGE_2 and decreased 15-keto-PGE_2. The level of COX-2 was not changed in Huh7 cells with stable overexpression or knockdown of 15-PGDH (Figure 4C). These observations are in accordance with the enzymatic action of 15-PGDH (converting PGE_2 to 15-keto-PGE_2). Consistent with activation of PPARγ by 15-keto-PGE_2 in 3T3-L1 fibroblasts(24), we observed that 15-PGDH overexpression in HCC cells increased PPARγ binding to PPRE (PPAR response element), whereas 15-PGDH knockdown reduced the PPARγ binding to PPRE, as determined by EMSA (Figure 4D) and by DNA pull down assay (Figure 4E). The involvement of 15-keto-PGE_2 in 15-PGDH-induced PPARγ-PPRE binding in HCC cells was supported by the observation that the effect was blocked by overexpression of PGR2 (15-oxoprostaglandin-Δ^{13}-reductase), which catalyzes the reaction converting 15-keto-PGE_2 to 13,14-dihydro-15-keto-PGE_2. Consistent

with these findings, we found that 15-PGDH overexpression increased PPRE luciferase reporter activity, whereas 15-PGDH knockdown reduced it (Figure 4F). The effect of 15-PGDH on PPRE reporter activity was abolished when PGR2 was overexpressed or when the cells were treated with 10μM GW9662, a PPARγ antagonist. Furthermore, treatment of wild type Huh7 cells with 15-keto-PGE_2 increased the PPRE reporter activity and the effect was abolished by PGR2 overexpression or by GW9662 treatment (10μM). Taken together, these results demonstrate that 15-PGDH-derived 15-keto-PGE_2 is able to activate PPARγ in HCC cells.

15-PGDH-derived 15-keto-PGE_2 induces $p21^{WAF1/Cip1}$ gene transcription through PPARγ

Given that 15-PGDH signaling increased $p21^{WAF1/Cip1}$ expression (see Figures 2, 3 and 5) and that PPARγ is a ligand-dependent transcription factor that regulates target gene expression through binding to PPRE, we postulated that PPARγ might be a key transcription factor that mediates 15-PGDH/15-keto-PGE_2-induced $p21^{WAF1/Cip1}$ expression in HCC cells. Indeed, sequence alignment analysis revealed the presence of PPRE consensus sequence [C(A/G)(A/G)A(A/T)CT] within the $p21^{WAF1/Cip1}$ promoter (−2151 to −2145, −1782 to −1188, −1186 to −1179, −1000 to −993). Consequently, we utilized a luciferase reporter construct driven by the p21 gene promoter (from –2192 to +10, containing the PPRE consensus sequences) to evaluate the impact of 15-PGDH/15-keto-PGE_2 on p21 promoter activity. As shown in Figure 5A, 15-PGDH overexpression increased p21 promoter luciferase reporter activity, whereas 15-PGDH knockdown reduced it; this effect was reversed by overexpression of PGR2 or by treatment with the PPARγ antagonist GW9662 (10μM). Accordingly, treatment of the wild type Huh7 cells with 15-keto-PGE_2 (10μM) significantly enhanced the p21 promoter reporter activity and this effect was abolished by PGR2 overexpression or GW9662 treatment (10μM). These findings suggest the involvement of PPARγ in 15-PGDH/15-keto-PGE_2-induced p21 gene transcription. Consistent with these results, chromatin immunoprecipitation (CHIP) assay showed that 15-PGDH overexpression enhanced the binding of PPARγ to p21 promoter DNA, whereas 15-PGDH knockdown reduced this interaction (Figure 5B and C). Overexpression of PGR2 reversed 15-PGDH-mediated interaction between PPARγ and p21 promoter DNA. Treatment of wild type Huh7 cells with 15-keto-PGE_2 (10μM) also enhanced PPARγ association with the p21 promoter DNA and the effect was blocked by the PPARγ antagonist GW9662 (10μM). Treatment of wild type Huh7 cells with the pharmacologic PPARγ agonist, ciglitazone, also increased PPARγ association with the p21 promoter (Figure 5D). These observations demonstrate that 15-PGDH-derived 15-keto-PGE_2 induces PPARγ association with the p21 promoter and enhances p21 transcription in HCC cells. This assertion is further supported by the western blot analyses showing that the p21 protein and phosphorylated p21 were increased in 15-PGDH overexpressed cells but decreased in 15-PGDH knockdown cells (Figure 5E). The 15-PGDH-induced increase of p21 protein and phosphorylated p21 was also influenced by PGR2 and PPARγ (attenuated by PGR2 overexpression or by PPARγ knockdown; enhanced by PPARγ overexpression). Taken together, these results establish an important role of PPARγ in 15-PGDH/15-keto-PGE_2-induced p21 expression in HCC cells.

The effect of 15-PGDH on p21$^{WAF1/Cip1}$ association with PCNA and CDKs in HCC cells

Consistent with the notion that p21 inhibits PCNA and CDKs in the nucleus, Western blotting analysis showed that 15-PGDH overexpression caused accumulation of p21 in the nucleus and decrease of p21 in the cytoplasm (Figure 6A). In contrast, 15-PGDH knockdown led to reduction of p21 in the nucleus and increase of p21 in the cytoplasm. Co-immunoprecipitation analysis showed that 15-PGDH overexpression increased the interaction between p21 and PCNA, whereas 15-PGDH knockdown inhibited their interaction (Figure 6B). In parallel, 15-PGDH overexpression also increased p21 interaction with CDK2, CyclinE, CDK4 and CyclinD1, whereas 15-PGDH knockdown inhibited these interactions (Figure 6C and 6D). Furthermore, 15-PGDH overexpression enhanced E2F1 binding to RB and decreased E2F1 binding to C-myc, while an opposite pattern of interactions was observed in cells with 15-PGDH knockdown (Figure 6E). These findings demonstrate that 15-PGDH signaling influences p21 interaction with key cell cycle-regulatory molecules.

Regulation of p21$^{WAF1/Cip1}$ by 15-PGDH is independent of p53 in HCC cells

Given that the expression of p21 in human cells is regulated by wild type p53, we performed further experiments to determine whether p53 is implicated in 15-PGDH-mediated regulation of p21 in HCC cells. To this end, we utilized HepG2 cell line that expresses wild type p53 (Huh7 cells have p53 mutation). Western blotting analysis showed that shRNA depletion of p53 did not alter 15-PGDH-induced p21 expression (nuclear accumulation and cytoplasmic reduction), despite that p53 depletion reduced p21 protein in cells without 15-PGDH overexpression (Figure 7A). Similarly, luciferase reporter activity assay showed that shRNA depletion of p53 did not alter 15-PGDH-induced p21 promoter activity, although p53 depletion reduced p21 promoter reporter activity in cells without 15-PGDH overexpression (Figure 7B). Furthermore, p53 depletion did not influence 15-PGDH-induced interaction of p21 with CDK2, CDK4, PCNA and the interaction between E2F1 and RB, although p53 depletion decreased the interactions of these molecules in cells without 15-PGDH overexpression (Figure 7C). Finally, CHIP assay showed that p53 depletion did not alter 15-PGDH-induced PPARγ binding to the p21 promoter DNA, although p53 depletion reduced their binding in cells without 15-PGDH overexpression (Figure 7D). These results suggest that 15-PGDH signaling upregulates p21 expression in HCC cells through mechanisms independent of p53.

p21$^{WAF1/Cip1}$ mediates the anti-tumor effect of 15-PGDH

To further evaluate the role of p21 in 15-PGDH-mediated anti-tumor effect, additional experiments were performed to determine whether overexpression or knockdown of p21 would influence 15-PGDH-regulated cell growth. As shown in Figure 8A, knockdown of p21 reversed 15-PGDH-induced inhibition of HCC cell proliferation and clonogeneic growth. On the other hand, overexpression of p21 prevented cell proliferation and clonogenic growth induced by 15-PGDH knockdown (Figure 8B). These results demonstrate a key role of p21 in 15-PGDH-mediated inhibition of HCC cell growth.

DISCUSSION

Recent studies suggest an emerging role of 15-PGDH in several non-hepatic cancers(15–23, 25–29). Reduction of 15-PGDH is associated with enhanced cell proliferation and is an independent predictor for poor survival in gastric adenocarcinoma(27). A haplotype in the 15-PGDH gene is positively associated with colorectal cancer risk(20). In mouse models of colonic carcinogenesis, overexpression of 15-PGDH decreases cancer cell growth or delays tumor formation, whereas deletion of 15-PGDH increases susceptibility to chemically or genetically induced colon tumors(16). Targeted adenovirus-mediated delivery of 15-PGDH gene inhibited colon cancer growth in a mouse xenograft model(30). The hepatocyte growth factor (HGF) and its receptor c-Met signaling promotes PGE_2 biogenesis in colorectal cancer cells via up-regulation of COX-2 and down-regulation of 15-PGDH(31). Reciprocal regulation between COX-2 and 15-PGDH expression has been documented in several cancers(32). Omega-3 polyunsaturated fatty acids reduce the level of PGE_2 in hepatocellular carcinoma and cholangiocarcinoma cells through down-regulation of COX-2 and induction of 15-PGDH(33, 34). Anti-cancer therapeutics, such as transforming growth factor (TGF)-β1, glucocorticoids and histone deacetylase (HDAC) inhibitors, have been shown to exert their anti-carcinogenic activity in part through induction of 15-PGDH expression(26, 35). All of these findings suggest a tumor suppressive function of 15-PGDH. However, to date, the action of 15-PGDH is largely attributable to its degradation of biologically active PGE_2, with its 15-keto metabolite being considered largely inactive. The current study provides paradigm-shifting evidence for an active role of 15-keto-PGE_2 in 15-PGDH-mediated inhibition of cancer cell growth. Our results reveal that 15-PGDH-derived 15-keto-PGE_2 is a natural PPARγ ligand which induces PPARγ association with $p21^{WAF1/Cip1}$ promoter and enhances p21 gene expression leading to inhibition of HCC growth (illustrated in Figure 9).

$p21^{WAF1/Cip1}$ is a potent inhibitor of cyclin-dependent kinases (CDKs). It inhibits cell cycle progression through binding to cyclin-cdk complexes(36–38). Association of p21 to cyclin-cdk complexes also prevents phosphorylation of the retinoblastoma (RB) protein thus preventing the release of E2F transcription factor(39). In addition, p21 also binds to proliferating cell nuclear antigen (PCNA) and interferes with PCNA-dependent DNA polymerase activity leading to inhibition of DNA replication(40). The growth-inhibitory action of p21 is attributed to the functions of the carboxy-terminal PCNA-binding domain as well as the amino-terminal CDK-cyclin inhibitory domain(41, 42). Consistent with the growth-inhibitory effect of p21, we have shown that 15-PGDH-derived 15-keto-PGE_2 induces p21 expression in HCC cells and this signaling pathway suppresses HCC cell growth. The role of p21 in 15-PGDH/15-keto-PGE_2-mediated inhibition of HCC cell growth is attested by the observations that p21 knockdown reversed 15-PGDH-induced inhibition of tumor cell growth and that overexpression of p21 prevented the cell growth induced by 15-PGDH knockdown.

PPARγ is a ligand-activated nuclear transcription factor regulating the expression of target genes by binding to PPRE in target genes(43, 44). The activity of PPARγ is regulated by several ligands, including thiazolidinediones (such as ciglitazone), 15-deoxy-$\Delta^{12,14}$ prostaglandin J_2 (15d-PGJ_2), and other fatty acid derivatives. Our results in the current study document a key role of PPARγ in mediating 15-PGDH/15-keto-PGE_2 actions in HCC cells.

We have shown that 15-PGDH-derived 15-keto-PGE_2 is an endogenous ligand that activates PPARγ in HCC cells. Evidences for activation of PPARγ by 15-PGDH-derived 15-keto-PGE_2 include: (1) 15-PGDH overexpression increased PPARγ binding to PPRE as determined by EMSA and DNA pulldown assays; (2) 15-PGDH knockdown reduced PPARγ binding to PPRE as determined by EMSA and DNA pulldown assays; (3) the effect of 15-PGDH on PPARγ-PPRE binding was blocked by overexpression of PGR2, an enzyme that converts 15-keto PGE_2 to 13,14-dihydro-15-keto PGE_2; (4) 15-PGDH overexpression increased PPRE luciferase reporter activity; (5) 15-PGDH knockdown reduced PPRE reporter activity; (6) the effect of 15-PGDH on PPRE reporter activity was abolished by overexpression of PGR2 or by treatment with the PPARγ antagonist GW9662; (7) 15-keto-PGE_2 increased PPRE reporter activity and the effect was abolished by PGR2 overexpression or by GW9662 treatment.

Another important finding in this study is that 15-PGDH-derived 15-keto-PGE_2 increases PPARγ association with p21 gene promoter thus enhancing p21 gene transcription. Evidences supporting the role of PPARγ in 15-PGDH/15-keto-PGE_2-induced p21 gene transcription include: (1) 15-PGDH overexpression increased PPARγ association with p21 promoter DNA and enhanced p21 luciferase reporter activity; (2) 15-PGDH knockdown decreased PPARγ association with p21 promoter DNA and reduced p21 luciferase reporter activity; (3) the effect of 15-PGDH on p21 promoter reporter activity and PPARγ binding was reversed by overexpression of PGR2 or by treatment with the PPARγ antagonist GW9662; (4) 15-keto-PGE_2 treatment increased p21 promoter reporter activity/PPARγ association and the effect was blocked by PGR2 overexpression or by GW9662 treatment; (5) 15-PGDH overexpression increased p21 protein whereas 15-PGDH knockdown decreased p21 protein; (6) the effect of 15-PGDH on p21 protein induction was influenced by PGR2 and PPARγ.

The results of this study depict a key 15-PGDH/15-keto-PGE_2/PPARγ/p21 signaling axis that suppresses hepatocarcinogenesis and tumor progression. Since 15-PGDH converts oncogenic PGE_2 to tumor suppressive 15-keto-PGE_2, induction of endogenous 15-PGDH expression or delivery of exogenous 15-PGDH/15-keto-PGE_2 may represent promising future therapeutic interventions. It is conceivable that this approach may provide more effective anti-tumor therapy with fewer side effects compared to the selective COX-2 inhibitors.

METHODS

Cell lines

Human HCC cell lines (Huh7 and HepG2) and murine HCC cell line (Hepa1-6) were obtained from ATCC. The cells were maintained in Minimum Essential Medium (MEM) (Gibco BRL Life Technologies) supplemented with 10% heat-inactivated (56°C, 30 minutes) fetal bovine serum (Sigma) in a humidified atmosphere of 5% CO_2 incubator at 37°C.

Selection of Huh stable cell lines

Huh7 cells were transfected with pCMV6-AC-GFP, pCMV6-AV-GFP-15PGDH, pGFP-V-RS, pGFP-V-RS-15PGDH using the transfection reagent Lipofectamine^{R} 2000 (Invitrogen) (the plasmid constructs were obtained from Origene, Rockville, MD). Forty-eight hours after transfection, the cells were cultured with the selection media containing 1-2 mg/ml G418 (Calbiochem) for 15-PGDH overexpression or 1-2 μg/ml Puromycin (Invitrogen) for 15-PGDH knockdown. The selection media were replaced every 3 days. Distinct colony of the surviving cells was transferred onto 96-well plate and the cells were continuously maintained in the selection media. The transfection efficiency was verified by immunofluorescence staining with anti-GFP antibody (1:200, Evrogen) and by Western blotting with anti-15-PGDH antibody (1:500, Santa Cruz Biotech).

To select cells with 15-PGDH overexpression plus p21 depletion, Huh7 cells stably transfected with the 15-PGDH expression vector (pCMV6-GFP-AC-15PGDH) were subsequently transfected with the p21 RNAi vector (pGFP-V-RS-WAF1/Cip1/p21, obtained from Origene, Rockville, MD). The double transfection cells were selected by using G418 and Puromycin.

To select cells with 15-PGDH knockdown plus p21 overexpression, the Huh7 cells stably transfected with the 15-PGDH RNAi vector (pGFP-V-RS-15PGDH) were subsequently transfected with the p21 expression vector (pcDNA3/WAF1/Cip1/p21, obtained from Addgene). The double transfection cells were selected by using Puromycin and G418.

Cell proliferation WST-1 assay

The cells were synchronized in G0 phase by serum deprivation and then released from growth arrest by reexposure to complete medium with serum. Cell proliferation was detected by reagent WST-1 kit (Roche) according to the manufacturer instruction. Cell growth curve was based on the normalized values of OD450 and each point represents the mean of three independent samples.

Cell cycle analysis

Cell cycle distribution was determined by using flow cytometry. 5×10^{6} cells in a 10 cm dish were grown overnight. Then the cells were then kept in serum-deprived medium for 48 h for synchronization to G0 phase. The cells were released from growth arrest by reexposure to 10% fetal bovine serum for 24 h. Cells were collected by trypsinization followed by centrifugation, washed once with PBS, and resuspended in 0.2 ml of ice-cold PBS. The collected cells were fixed in 70% cold ethanol [in 50 mM glycine buffer (pH 2.0)] overnight at −20°C. 100 μg/ml RNase A (Qiagen) was added to the cells with incubation for 30 minutes at 37°C. The cells were resuspended in 0.5 ml 100μg/ml propidium iodide (PI) solution (Borhoringer Nannheim Co.) for staining. The stained cells were analyzed by a FACScan Flow Cytometer at the LCRC FACS core facility. The percentage of cells in S, G0/G1, and G2/M phases of the cell cycle was determined using EXPO32 Cell Quest software. All experiments were conducted in triplicate.

BrdU staining

80% confluent cells were cultured for 24 hour before treatment with 10μl BrdU (Roche) for 4 hours. Immunofluorescent staining with an anti-BrdU antibody (1:100, Santa Cruz Biotech) was performed according to the manufacturer's instructions (Becton Dickinson). TRITC fluorescent conjugated secondary antibody (1:200, Abcam) was utilized to visualize the anti-BrdU labeled cells.

Soft agar colony formation assay

10^3 cells were plated on a 10-cm dish containing 0.5% (down) and 0.35% (up) double layer soft-agar. The dishes were incubated at 37°C in humidified incubator for 21 days. The cells were fed 1–2 times per week with DMEM (Gibco BRL Life Technologies). The colonies were stained with 2.5 ml of 0.005% Crystal Violet (Sigma) for more than 1 hour and the numbers of colonies were tallied.

Chromatin immunoprecipitation

Formaldehyde cross-linking and chromatin immunoprecipitation assays are performed according to the protocol provided by Upstate Biotechnology with modifications. The WAF1/Cip1/p21 promoter PCR primer sequences are: P1: 5'-GTGGCTCTGATTGGCTTTCTG-3'; P2: 5'-CTGAAAACAGGCAGCCCAAG-3'. Additional details are described in the Supplementary Materials and Methods.

DNA pull down

Cells were lysed by sonication in HKMG buffer (10 mM HEPES, PH7.9, 100 mM KCl, 5 mM $MgCl_2$, 100% glycerol, 1 mM DTT, and 0.5% NP40) containing protease and phosphatase inhibitors for the preparation of nuclear exact. The nuclear extracts were precleared with Streptavidin-agarose Resin (Thermo) for 1 hour and then incubated with 1μg of biotinylated double-stranded oligonucleotides (corresponding to the PPRE consensus site in the p21 promoter): P1:5'-Biotin-AGGTCACTGGTCA-3'; P2:5'-TGACCAGTGACC-3' (synthesized by Integrated DNA Technologies, USA), along with 10μg of poly(dI-dC) (Sigma) for 24 hours. DNA-bound proteins were collected with streptavidin-agarose resin and the samples were subjected to SDS-PAGE and Western blotting analysis.

Luciferase reporter assay

Cells (1×10^5 per well in six-well plate) were transiently transfected with 1 μg of luciferase construct (pGL3-PPRE or pGL3-WAF1/Cip1/p21 promoter) and 0.1 μg of pRL-Tk (Addgene) using Lipofectiamine^{TM} 2000 (Invitrogen) (with additionally plasmids as indicated). 36 hours after transfection, the cells were harvested with lysis buffer and luciferase activities of the cell extracts were measured using the dual luciferase assay system (Promega). The luciferase activity was normalized for transfection efficiency with Renilla luciferase activity.

Xenograft tumor study in SCID mice

Four-week male athymic NOD CB17-prkdc/SCID (severe combined immunodeficiency) mice were purchased from Jackson laboratory and maintained in the animal facilities

according to the protocol approved by the American Association for Accreditation of Laboratory Animal Care. Six athymic SCID mice per group were injected subcutaneously at the armpit area with Huh7 cells stably transfected with pCMV6-AC-GFP, pCMV6-AV-GFP-15PGDH, pGFP-V-RS, pGFP-V-RS-15PGDH, respectively (1×10^8 cells in 100μl of PBS). The mice were observed over 4 weeks and then sacrificed to recover the tumors. The wet weight of each tumor was determined. Portion of the tissue from each tumor was snap-frozen. Additional portion of each tumor was fixed in 4% paraformaldehyde and embedded in paraffin for hematoxylin and eosin (H&E) stain and for PCNA immunostain.

Xenograft tumor study in C57BL/6J mice

Mouse HCC cell line (Hepa1-6) (1×10^8 cells in 0.2 ml of PBS) was inoculated subcutaneously at armpit into syngenetic C57BL/6J mice. The mice were divided into two groups and subjected to intratumoral injection of pAd or pAd-15-PGDH (10^{10} pfu). The diameters of the tumors were measured every three days and the tumor volume was calculated using the formula $V=L/2*w^2$. The mice were sacrificed 31 days after inoculation to recover the tumor tissue. The wet weight of each tumor was determined for each mouse. A portion of the tissue from each tumor was snap-frozen. Additional portion of each tumor was fixed in 4% paraformaldehyde and embedded in paraffin for hematoxylin and eosin (H&E) stain and for PCNA immunostain.

Statistical analysis

The values are presented as mean±standard error of the mean (SEM) unless otherwise noted, with a minimum of three replicates. The results were evaluated by SPSS12.0 statistical soft and Student's t-test was used for comparisons, with $p < 0.05$ considered significant.

Supplementary Material

Refer to Web version on PubMed Central for supplementary material.

ACKNOWLEDGEMENT

The authors thank Dr. Hsin-Hsiung Tai at the University of Kentucky for providing the 15-PGDH-adenoviral vector.

Supported by National Institutes of Health grants CA102325, CA106280, CA134568 and DK077776.

ABBREVIATIONS

15-PGDH	15-hydroxyprostaglandin dehydrogenase
15-keto-PGE$_2$	15-keto-prostaglandin E_2
CDK	cyclin dependent kinase
CHIP	chromatin immunoprecipitation
COX-2	cyclooxygenase-2
EMSA	Electrophoretic mobility shift assay

HCC	hepatocellular carcinoma
IP	immunoprecipitation
PCNA	proliferating cell nuclear antigen
PGE_2	prostaglandin E_2
PGR	15-oxoprostaglandin-Δ^{13}-reductase
PPARγ	peroxisome proliferator activated receptor-γ
PPRE	peroxisome proliferator response element
SCID	severe combined immunodeficiency

REFERENCES

1. El-Serag HB. Hepatocellular carcinoma. N Engl J Med. 2011 Sep 22; 365(12):1118–1127. [PubMed: 21992124]
2. El-Serag HB. Epidemiology of viral hepatitis and hepatocellular carcinoma. Gastroenterology. 2012 May; 142(6):1264–1273. e1. [PubMed: 22537432]
3. Farazi PA, DePinho RA. Hepatocellular carcinoma pathogenesis: from genes to environment. Nat Rev Cancer. 2006 Sep; 6(9):674–687. [PubMed: 16929323]
4. Llovet JM, Bruix J. Molecular targeted therapies in hepatocellular carcinoma. Hepatology. 2008 Oct; 48(4):1312–1327. [PubMed: 18821591]
5. Wu T. Cyclooxygenase-2 in hepatocellular carcinoma. Cancer Treat Rev. 2006 Feb; 32(1):28–44. [PubMed: 16337744]
6. Breinig M, Schirmacher P, Kern MA. Cyclooxygenase-2 (COX-2)--a therapeutic target in liver cancer? Curr Pharm Des. 2007; 13(32):3305–3315. [PubMed: 18045183]
7. Cervello M, Montalto G. Cyclooxygenases in hepatocellular carcinoma. World J Gastroenterol. 2006 Aug 28; 12(32):5113–5121. [PubMed: 16937518]
8. Claria J, Kent JD, Lopez-Parra M, Escolar G, Ruiz-Del-Arbol L, Gines P, et al. Effects of celecoxib and naproxen on renal function in nonazotemic patients with cirrhosis and ascites. Hepatology. 2005 Mar; 41(3):579–587. [PubMed: 15723448]
9. Bosch-Marce M, Claria J, Titos E, Masferrer JL, Altuna R, Poo JL, et al. Selective inhibition of cyclooxygenase 2 spares renal function and prostaglandin synthesis in cirrhotic rats with ascites. Gastroenterology. 1999 May; 116(5):1167–1175. [PubMed: 10220509]
10. Vanchieri C. Vioxx withdrawal alarms cancer prevention researchers. J Natl Cancer Inst. 2004 Dec 1; 96(23):1734–1735. [PubMed: 15572751]
11. Couzin J. Clinical trials. Nail-biting time for trials of COX-2 drugs. Science. 2004 Dec 3; 306(5702):1673–1675. [PubMed: 15576585]
12. Grosser T, Fries S, FitzGerald GA. Biological basis for the cardiovascular consequences of COX-2 inhibition: therapeutic challenges and opportunities. J Clin Invest. 2006 Jan; 116(1):4–15. [PubMed: 16395396]
13. Baron JA, Sandler RS, Bresalier RS, Quan H, Riddell R, Lanas A, et al. A randomized trial of rofecoxib for the chemoprevention of colorectal adenomas. Gastroenterology. 2006 Dec; 131(6): 1674–1682. [PubMed: 17087947]
14. Tai HH. Prostaglandin catabolic enzymes as tumor suppressors. Cancer Metastasis Rev. 2011 Dec; 30(3–4):409–417. [PubMed: 22020925]
15. Kaliberova LN, Kusmartsev SA, Krendelchtchikova V, Stockard CR, Grizzle WE, Buchsbaum DJ, et al. Experimental cancer therapy using restoration of NAD+ -linked 15-hydroxyprostaglandin dehydrogenase expression. Mol Cancer Ther. 2009 Nov; 8(11):3130–3139. [PubMed: 19887544]

16. Myung SJ, Rerko RM, Yan M, Platzer P, Guda K, Dotson A, et al. 15-Hydroxyprostaglandin dehydrogenase is an in vivo suppressor of colon tumorigenesis. Proc Natl Acad Sci U S A. 2006 Aug 8; 103(32):12098–12102. [PubMed: 16880406]
17. Yan M, Myung SJ, Fink SP, Lawrence E, Lutterbaugh J, Yang P, et al. 15-Hydroxyprostaglandin dehydrogenase inactivation as a mechanism of resistance to celecoxib chemoprevention of colon tumors. Proc Natl Acad Sci U S A. 2009 Jun 9; 106(23):9409–9413. [PubMed: 19470469]
18. Tseng-Rogenski S, Gee J, Ignatoski KW, Kunju LP, Bucheit A, Kintner HJ, et al. Loss of 15-hydroxyprostaglandin dehydrogenase expression contributes to bladder cancer progression. Am J Pathol. 2010 Mar; 176(3):1462–1468. [PubMed: 20093479]
19. Liu Z, Wang X, Lu Y, Han S, Zhang F, Zhai H, et al. Expression of 15-PGDH is downregulated by COX-2 in gastric cancer. Carcinogenesis. 2008 Jun; 29(6):1219–1227. [PubMed: 18174234]
20. Frank B, Hoeft B, Hoffmeister M, Linseisen J, Breitling LP, Chang-Claude J, et al. Association of hydroxyprostaglandin dehydrogenase 15-(NAD) (HPGD) variants and colorectal cancer risk. Carcinogenesis. 2011 Feb; 32(2):190–196. [PubMed: 21047993]
21. Wolf I, O'Kelly J, Rubinek T, Tong M, Nguyen A, Lin BT, et al. 15-hydroxyprostaglandin dehydrogenase is a tumor suppressor of human breast cancer. Cancer Res. 2006 Aug 1; 66(15): 7818–7823. [PubMed: 16885386]
22. Huang G, Eisenberg R, Yan M, Monti S, Lawrence E, Fu P, et al. 15-Hydroxyprostaglandin dehydrogenase is a target of hepatocyte nuclear factor 3beta and a tumor suppressor in lung cancer. Cancer Res. 2008 Jul 1; 68(13):5040–5048. [PubMed: 18593902]
23. Ding Y, Tong M, Liu S, Moscow JA, Tai HH. NAD+-linked 15-hydroxyprostaglandin dehydrogenase (15-PGDH) behaves as a tumor suppressor in lung cancer. Carcinogenesis. 2005 Jan; 26(1):65–72. [PubMed: 15358636]
24. Chou WL, Chuang LM, Chou CC, Wang AH, Lawson JA, FitzGerald GA, et al. Identification of a novel prostaglandin reductase reveals the involvement of prostaglandin E2 catabolism in regulation of peroxisome proliferator-activated receptor gamma activation. J Biol Chem. 2007 Jun 22; 282(25):18162–18172. [PubMed: 17449869]
25. Backlund MG, Mann JR, Holla VR, Buchanan FG, Tai HH, Musiek ES, et al. 15-Hydroxyprostaglandin dehydrogenase is down-regulated in colorectal cancer. J Biol Chem. 2005 Feb 4; 280(5):3217–3223. [PubMed: 15542609]
26. Backlund MG, Mann JR, Holla VR, Shi Q, Daikoku T, Dey SK, et al. Repression of 15-hydroxyprostaglandin dehydrogenase involves histone deacetylase 2 and snail in colorectal cancer. Cancer Res. 2008 Nov 15; 68(22):9331–9337. [PubMed: 19010907]
27. Tatsuwaki H, Tanigawa T, Watanabe T, Machida H, Okazaki H, Yamagami H, et al. Reduction of 15-hydroxyprostaglandin dehydrogenase expression is an independent predictor of poor survival associated with enhanced cell proliferation in gastric adenocarcinoma. Cancer Sci. 2010 Feb; 101(2):550–558. [PubMed: 19917058]
28. Wakimoto N, Wolf I, Yin D, O'Kelly J, Akagi T, Abramovitz L, et al. Nonsteroidal anti-inflammatory drugs suppress glioma via 15-hydroxyprostaglandin dehydrogenase. Cancer Res. 2008 Sep 1; 68(17):6978–6986. [PubMed: 18757412]
29. Thiel A, Ganesan A, Mrena J, Junnila S, Nykanen A, Hemmes A, et al. 15-hydroxyprostaglandin dehydrogenase is down-regulated in gastric cancer. Clin Cancer Res. 2009 Jul 15; 15(14):4572–4580. [PubMed: 19584167]
30. Eruslanov E, Kaliberov S, Daurkin I, Kaliberova L, Buchsbaum D, Vieweg J, et al. Altered expression of 15-hydroxyprostaglandin dehydrogenase in tumor-infiltrated CD11b myeloid cells: a mechanism for immune evasion in cancer. J Immunol. 2009 Jun 15; 182(12):7548–7557. [PubMed: 19494278]
31. Moore AE, Greenhough A, Roberts HR, Hicks DJ, Patsos HA, Williams AC, et al. HGF/Met signalling promotes PGE(2) biogenesis via regulation of COX-2 and 15-PGDH expression in colorectal cancer cells. Carcinogenesis. 2009 Oct; 30(10):1796–1804. [PubMed: 19638428]
32. Tong M, Ding Y, Tai HH. Reciprocal regulation of cyclooxygenase-2 and 15-hydroxyprostaglandin dehydrogenase expression in A549 human lung adenocarcinoma cells. Carcinogenesis. 2006 Nov; 27(11):2170–2179. [PubMed: 16632868]

33. Lim K, Han C, Xu L, Isse K, Demetris AJ, Wu T. Cyclooxygenase-2-derived prostaglandin E2 activates beta-catenin in human cholangiocarcinoma cells: evidence for inhibition of these signaling pathways by omega 3 polyunsaturated fatty acids. Cancer Res. 2008 Jan 15; 68(2):553–560. [PubMed: 18199552]

34. Lim K, Han C, Dai Y, Shen M, Wu T. Omega-3 polyunsaturated fatty acids inhibit hepatocellular carcinoma cell growth through blocking beta-catenin and cyclooxygenase-2. Mol Cancer Ther. 2009 Nov; 8(11):3046–3055. [PubMed: 19887546]

35. Yang L, Amann JM, Kikuchi T, Porta R, Guix M, Gonzalez A, et al. Inhibition of epidermal growth factor receptor signaling elevates 15-hydroxyprostaglandin dehydrogenase in non-small-cell lung cancer. Cancer Res. 2007; 67(12):5587–5593. [PubMed: 17575121]

36. Abbas T, Dutta A. p21 in cancer: intricate networks and multiple activities. Nat Rev Cancer. 2009 Jun; 9(6):400–414. [PubMed: 19440234]

37. Starostina NG, Kipreos ET. Multiple degradation pathways regulate versatile CIP/KIP CDK inhibitors. Trends Cell Biol. 2012 Jan; 22(1):33–41. [PubMed: 22154077]

38. Jung YS, Qian Y, Chen X. Examination of the expanding pathways for the regulation of p21 expression and activity. Cell Signal. 2010 Jul; 22(7):1003–1012. [PubMed: 20100570]

39. Dotto GP. p21WAF1/CIP1: more than a break to the cell cycle? Biochemica Et Biophysica Acta. 2000; 1471 M43-M56] 2000(1471):M43-M56.

40. Rousseau D, Cannella D, Boulairs J, Fitzgerald P, Fotedar A, Fotedar R. Growth inhibition of CDK-cyclin and PCNA binding domains by p21 occurs by distinct mechanisms and is regulated by ubiquitinproteasome pathways. Oncogene. 1999; 18:4313. [PubMed: 10439039]

41. Chen J, Jackson PK, Kirschner MW, Dutta A. Separate domains of p21 involved in the inhibition of Cdk kinase and PCNA. Nature. 1995 Mar 23; 374(6520):386–388. [PubMed: 7885482]

42. Luo Y, Hurwitz J, Massague J. Cell-cycle inhibition by independent CDK and PCNA binding domains in p21Cip1. Nature. 1995 May 11; 375(6527):159–161. [PubMed: 7753174]

43. Kawai M, Rosen CJ. PPARgamma: a circadian transcription factor in adipogenesis and osteogenesis. Nat Rev Endocrinol. 2010 Nov; 6(11):629–636. [PubMed: 20820194]

44. Tontonoz P, Spiegelman BM. Fat and beyond: the diverse biology of PPARgamma. Annu Rev Biochem. 2008; 77:289–312. [PubMed: 18518822]

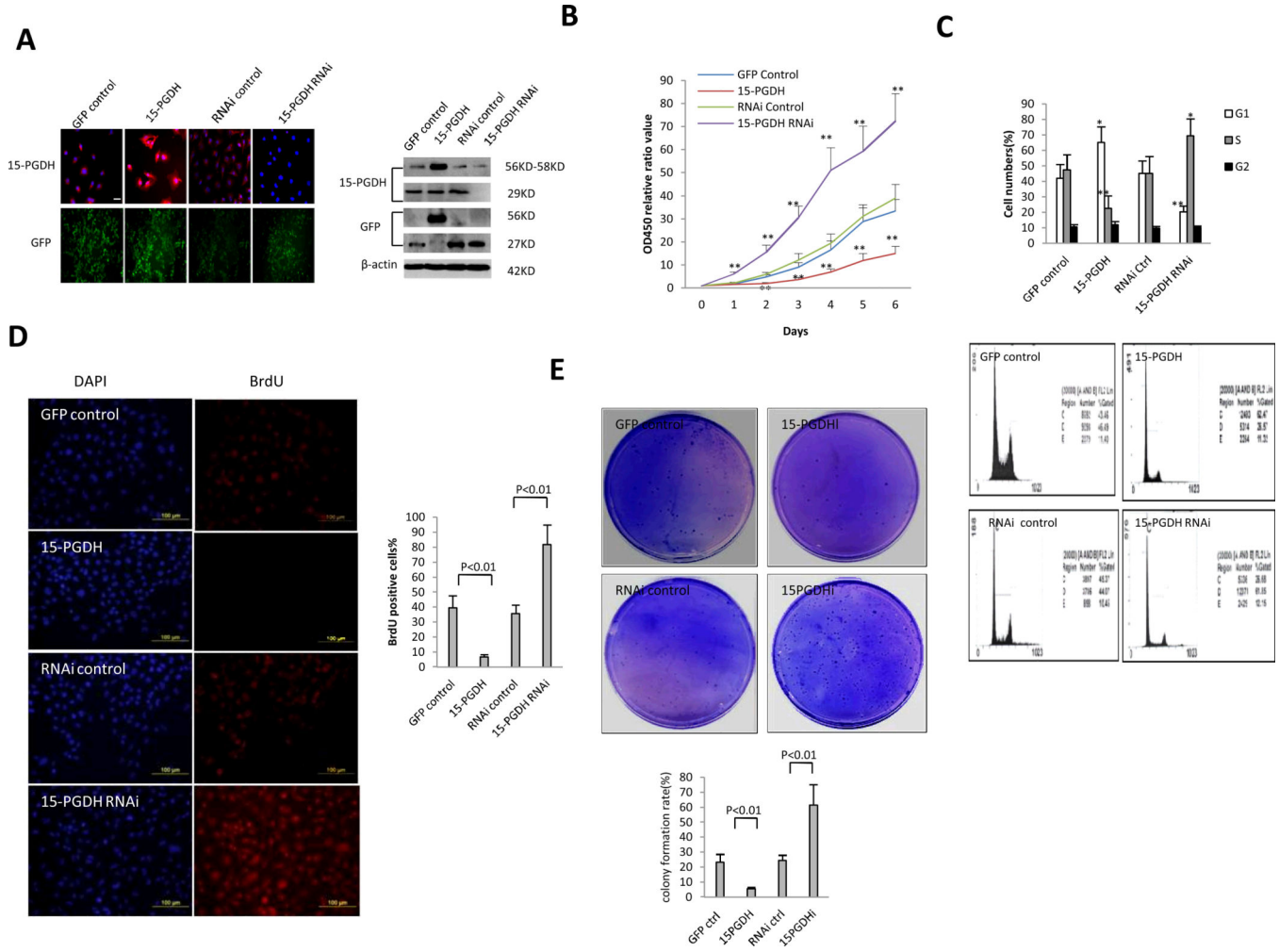

Figure 1. The effect of 15-PGDH on HCC cell growth, *in vitro*

A. Immunofluorescence (*Left*) and Western blotting (*Right*) for 15-PGDH in Huh7 cells with stable overexpression or knockdown of 15-PGDH.

B. Cell proliferation assay *in vitro*. WST proliferation assay was performed in 96-well plates. Each sample was assayed in triplicate for 6 consecutive days. The data represent mean±SEM from three experiments (**p < 0.01; *p < 0.05).

C. Cell cycle analysis by flow cytometry. The percentage of cells in the S, G1, and G2 phases of the cell cycle was determined using Cell EXPO32 software. The experiments were conducted in triplicate and the data are presented as mean±SEM (*p < 0.05; **p < 0.01).

D. BrdU immunofluorescence staining. (*Upper panel*) Representative photographs of BrdU positive cells from different groups are shown (scale bar 100 μm). (*Lower panel*) Quantitative analysis of BrdU positive cells.

E. Soft-Agar colony-formation efficiency assay. (*Upper panel*) Representative photographs of colony formation in soft agar plates. (*Lower panel*) Bar graph of colony formation rates. The data were from three independent experiments.

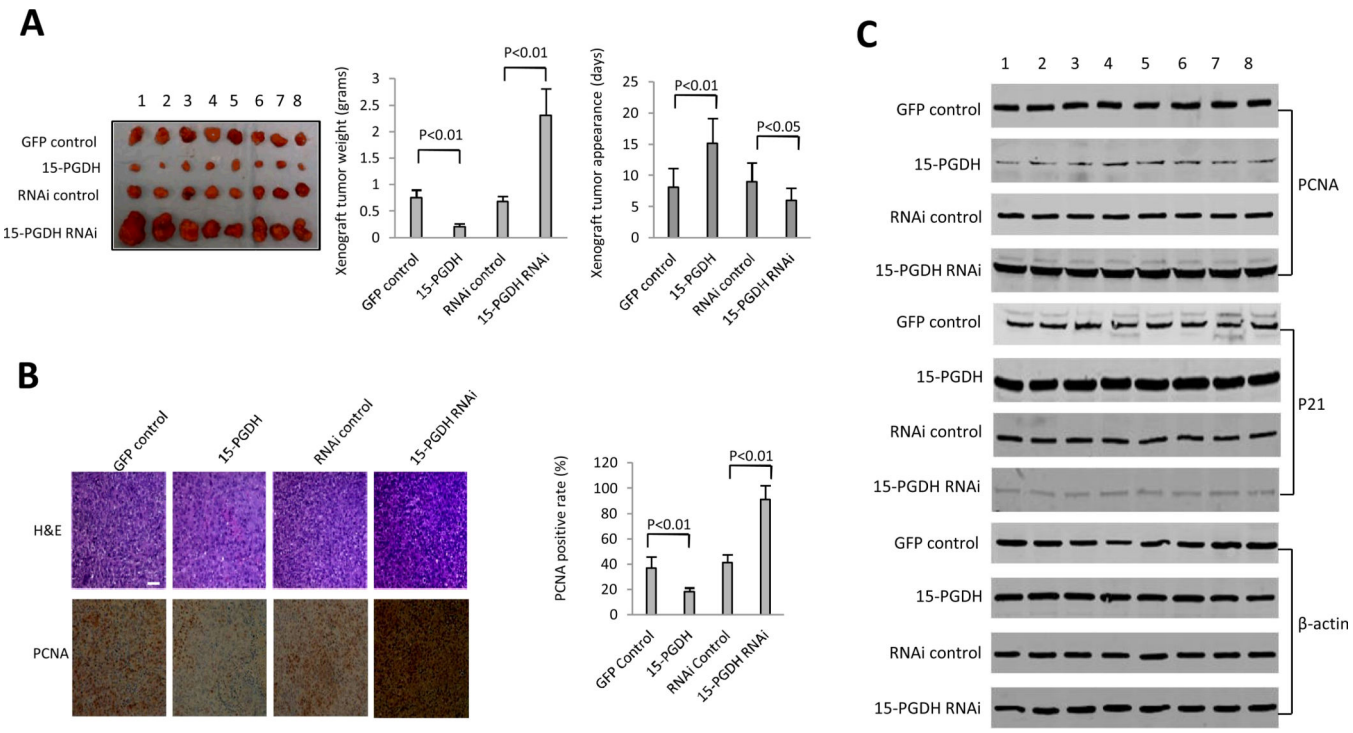

Figure 2. The effect of 15-PGDH on HCC growth in SCID mice

A. Tumorigenecity assay. Huh7 cells (1×10^8 cells in 0.2 ml of PBS) were injected subcutaneously at armpit in SCID mice. The mice were sacrificed 4 weeks after inoculation and the tumors were recovered. The wet weight of each tumor and tumor appearance time (days) were determined for each mouse. (*Left panel*) Photograph of xenograft tumors recovered from four groups of SCID mice inoculated with Huh7 cell lines (GFP control, 15-PGDH, RNAi control, 15-PGDH RNAi). (*Mid panel*) Xenograft tumor weights (grams). The data represent mean±SEM from eight SCID mice in each group. (*Right panel*) Xenograft tumors onset time (days). The data represent mean±SEM (n=8 for each group).

B. Immunohistochemical analysis of xenograft tumor tissues. (*Left panel*) Hematoxylin-eosin (H&E) stain and PCNA immunostain were performed in formalin-fixed, paraffin-embedded xenograft tumor tissues recovered from SCID mice (original magnification ×100). (*Right panel*) Semi-quantification of PCNA positive cells (the data represent mean ±SEM, n=8).

C. Western blotting for PCNA and p21 in xenograft tumors (8 samples each group). β-actin was used as the internal control.

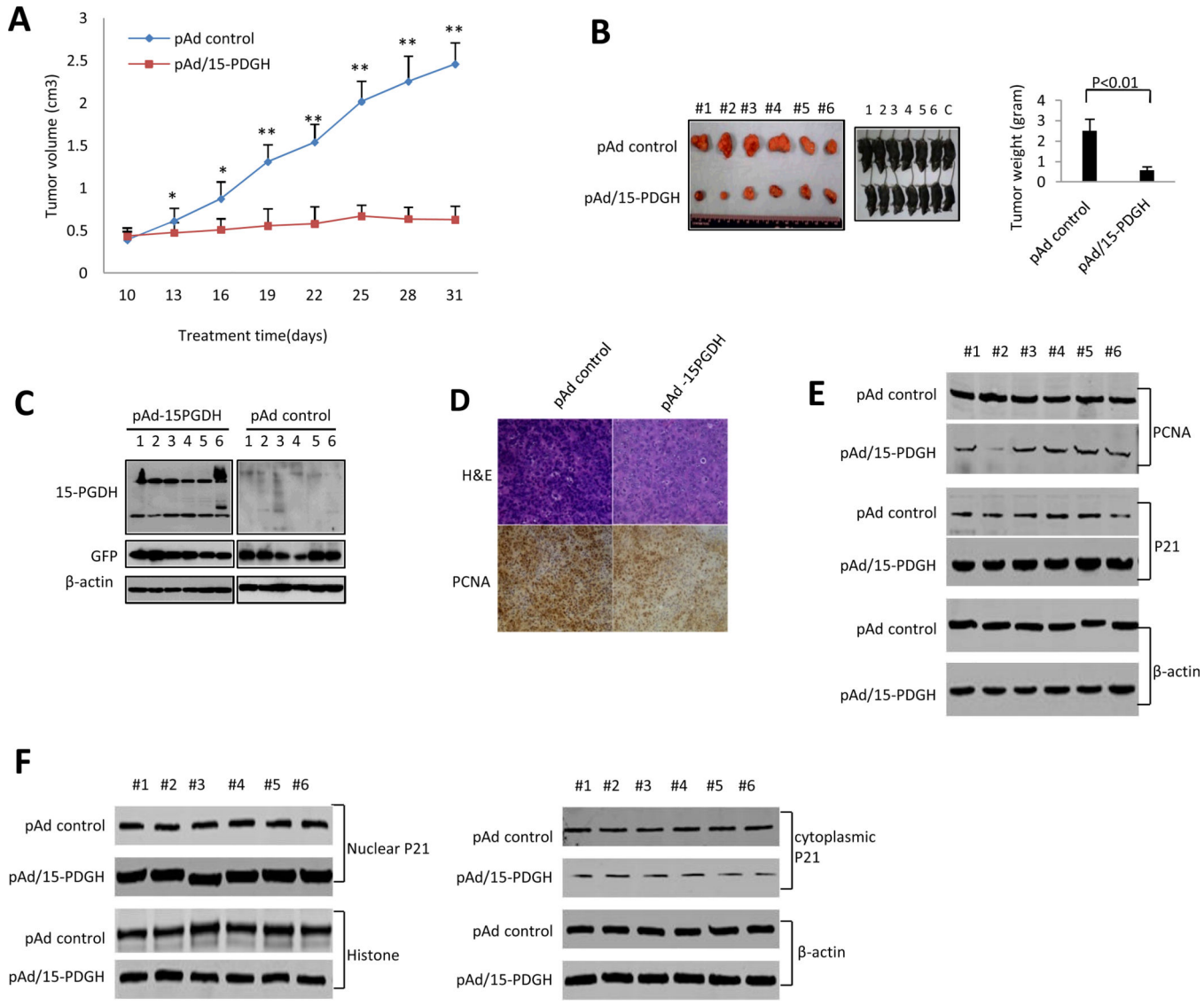

Figure 3. The effect of 15-PGDH on HCC growth in syngeneic C57BL/6J mice

Hepa1-6 cells (1×10^8 cells in 0.2 ml of PBS) were inoculated subcutaneously at armpit in C57BL/6J mice. When the tumor nodules become palpable, the pAd control virus or pAd-15-PGDH (10^{10} pfu) was injected directly to the tumor nodules (the injection was performed every three days, from the 10^{th} day to the 28^{th} day). After the last injection, the mice were observed for additional 3 days before sacrifice to recover tumor nodules. The wet weight of each tumor was recorded. The tumor diameters were measured by a caliper in two dimensions. The tumor volume was calculated by using the formula $V=L/2*w^2$.

A. Tumor size at different days. The data represent mean±SEM (n=6; *p < 0.05; **p < 0.01).

B. (*Left panels*) Photographs of C57BL/6J mice inoculated with Hepa1-6 cells (prior to sacrifice) and the recovered xenograft tumors. (*Right panel*) The average tumor weight. The data represent mean±SEM (n= 6).

C. Western blotting analysis for 15-PGDH in pAd-15-PGDH and pAd treated Hepa1-6 tumor tissues. β-actin was used as the internal control.
D. H&E stain and PCNA immunostain in pAd-15-PGDH and pAd treated Hepa1-6 tumors.
E. Western blotting for PCNA and p21 in pAd-15-PGDH and pAd treated Hepa1-6 tumors (6 samples for each group). β-actin was used as the internal control.
F. (*Left panel*) Western blotting to detect nuclear p21 in pAd-15-PGDH and pAd treated Hepa1-6 tumors (6 samples for each group). Histone was used as the internal control. (*Right panel*) Western blotting to detect cytoplasmic p21 in pAd-15-PGDH and pAd treated Hepa1-6 tumors (6 samples for each group). β-actin was used as the internal control.

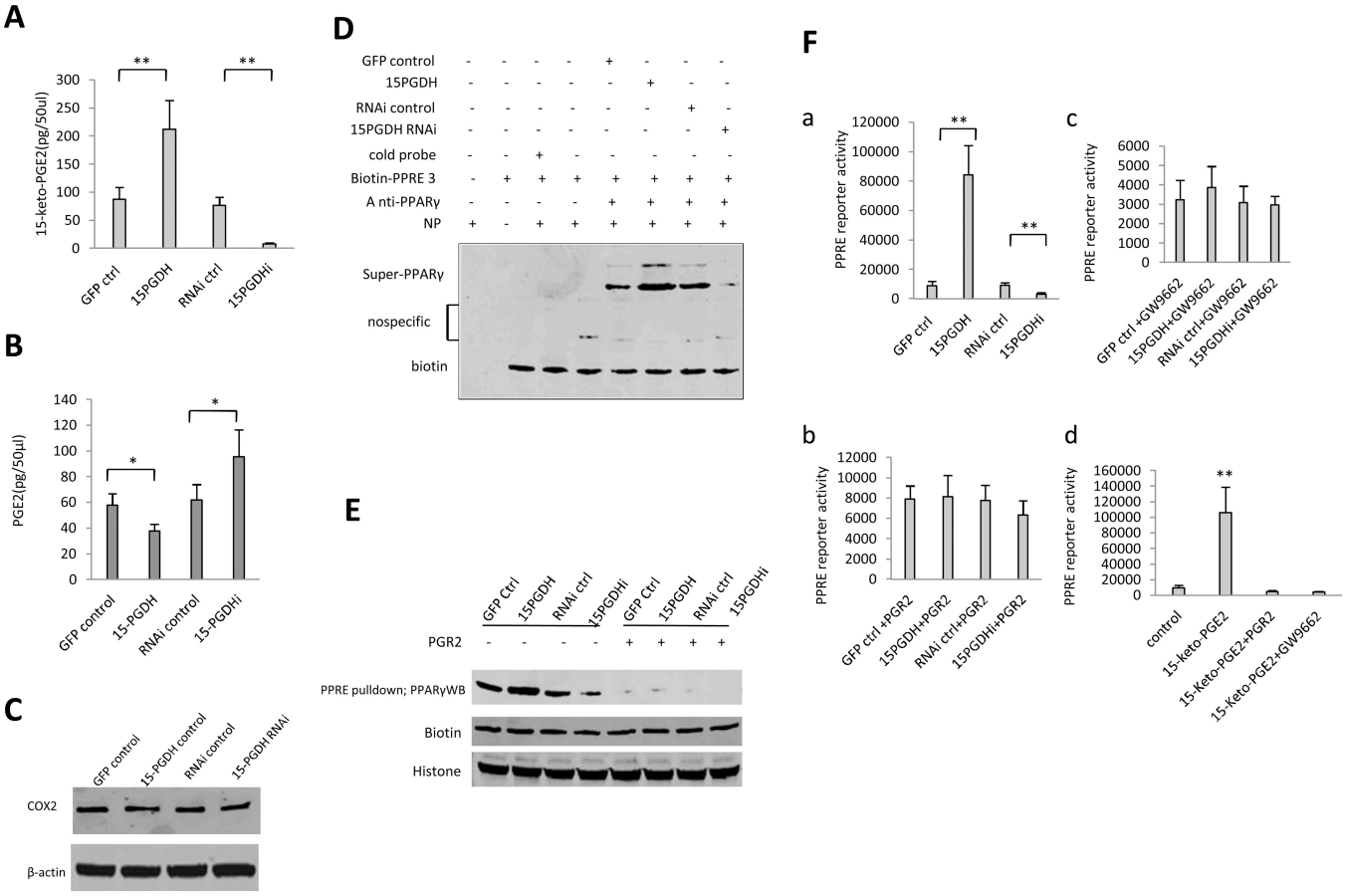

Figure 4. 15-PGDH-derived 15-keto-PGE$_2$ activates PPARγ in HCC cells

A. Enzyme immunoassay (EIA) for 15-keto-PGE$_2$ metabolite in Huh7 stable cell lines. The data are presented as mean±SEM (**p < 0.01 compared to corresponding control).

B. Enzyme immunoassay (EIA) for PGE$_2$ in Huh7 stable cell lines. The data are presented as mean±SEM (*p < 0.05; **p < 0.01).

C. Western blotting for COX-2 in Huh7 cells with stable overexpression or knockdown of 15-PGDH. β-actin was used as the internal control.

D. PPARγ super-EMSA analysis using PPRE probe in Huh7 stable cell lines.

E. DNA pulldown in Huh7 stable cell lines. Biotin and histone were used as pulldown and loading controls.

F. PPRE-luciferase activity assay. *a* PPRE luciferase reporter activity in Huh7 stable cell lines (**p < 0.01 compared to corresponding control). *b* PPRE luciferase reporter activity in Huh7 stable cell lines with cotransfection of pCMV6-entry-PGR2 (Origene). *c* PPRE luciferase reporter activity in Huh7 stable cell lines treated with GW9662 (10μM). *d* PPRE luciferase reporter activity in wild type Huh7 cells treated with DMSO and 15-keto-PGE$_2$ (10μM, Cayman Chemicals) (with or without PGR2 overexpression or 10μM GW9662 treatment).

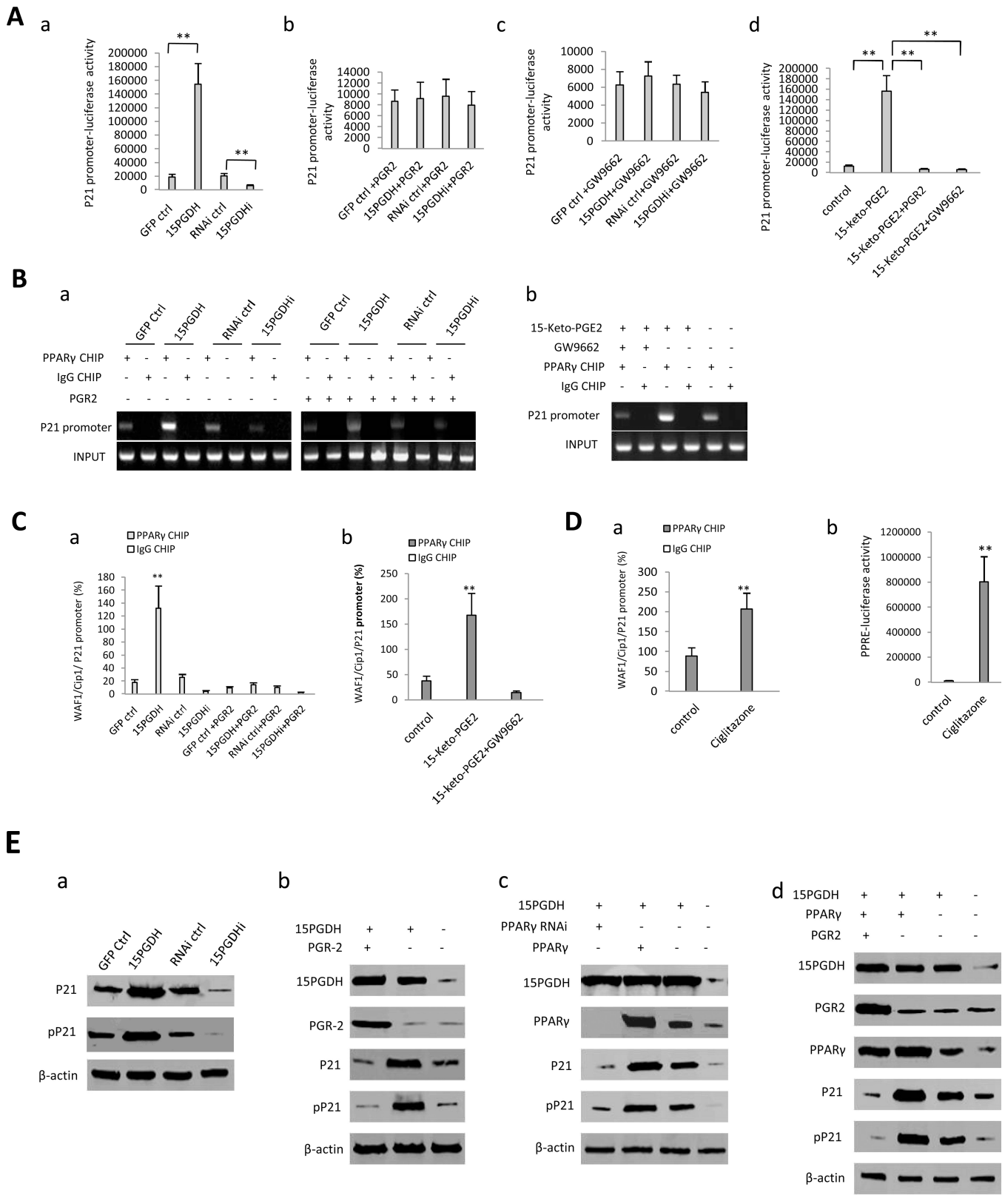

Figure 5. 15-PGDH-derived 15-keto-PGE$_2$ enhances PPARγ association with the p21 promoter and induces p21 expression in HCC cells

A. The effect of 15-PGDH and 15-keto-PGE_2 on p21 promoter activity. *a* p21 promoter luciferase reporter activity in Huh7 cells with altered expression of 15-PGDH (**$p < 0.01$). *b* p21 promoter luciferase reporter activity in Huh7 stable cell lines with co-transfection of PGR2. *c* p21 promoter luciferase reporter activity in Huh7 stable cell lines treated with 10μM GW9662. *d* 15-keto-PGE_2 (10μM) enhanced p21 promoter luciferase reporter activity in wild type Huh7 cells; the effect was abolished by PGR2 overexpression or by GW9662 treatment (10μM).

B. PPARγ CHIP-PCR assay. *a* PPARγ association with p21 promoter in Huh7 stable cells with or without PGR2 overexpression. *b* 15-keto-PGE_2 (10μM) enhanced PPARγ binding to the p21 promoter in wild type Huh7 cells and the effect was abolished by PGR2 overexpression or GW9662 treatment (10μM). IgG CHIP was used as the negative control. p21 promoter PCR product was used as the input.

C. PPARγ CHIP-real-time PCR assay. *a* PPARγ association with p21 promoter in Huh7 stable cells with or without PGR2 overexpression. *b* 15-keto-PGE_2 (10μM) enhanced PPARγ binding to the p21 promoter in wild type Huh7 cells and the effect was abolished by GW9662 treatment (10μM). IgG CHIP was used as the negative control.

D. Effect of the PPARγ agonist ciglitazone (10μM) in wild type Huh7 cells. *a* PPARγ CHIP-real-time PCR assay. *b* PPRE luciferase reporter activity assay.

E. Western blotting for p21 and phosphorylated p21 in Huh7 cells with indicated transfections.

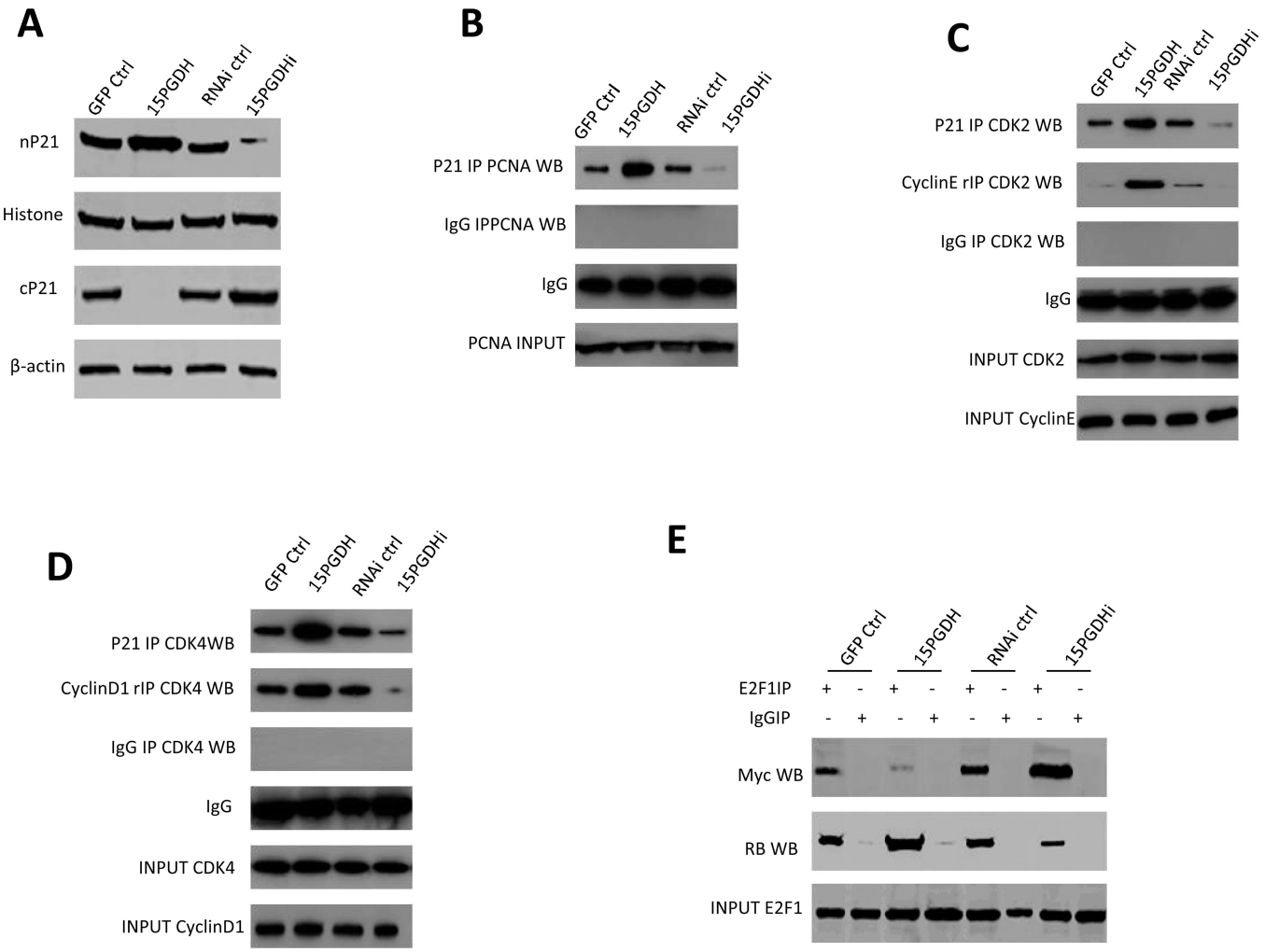

Figure 6. The effect of 15-PGDH signaling on p21 downstream molecules in HCC cells

A. Western blotting for p21 in the nuclear fraction (nP21) and p21 in the cytoplasmic fraction (cP21) from Huh7 stable cell lines with altered 15-PGDH expression. Histone and β-actin were used as the internal control, respectively.

B. Co-immunoprecipitation and western blotting analysis using indicated antibodies in Huh7 stable cell lines with altered 15-PGDH expression. IgG IP was used as the negative control. PCNA western blotting was used as input control.

C. Co-immunoprecipitation and western blotting analysis using indicated antibodies in Huh7 stable cell lines with altered 15-PGDH expression. IgG IP was used as the negative control. rIP denotes repeat co-immunoprecipitation.

D. Co-immunoprecipitation and western blotting analysis using indicated antibodies in Huh7 stable cell lines with altered 15-PGDH expression. IgG IP was used as the negative control. rIP denotes repeat co-immunoprecipitation.

E. Co-immunoprecipitation and western blotting analysis using indicated antibodies in Huh7 stable cell lines with altered 15-PGDH expression. IgG IP was used as the negative control.

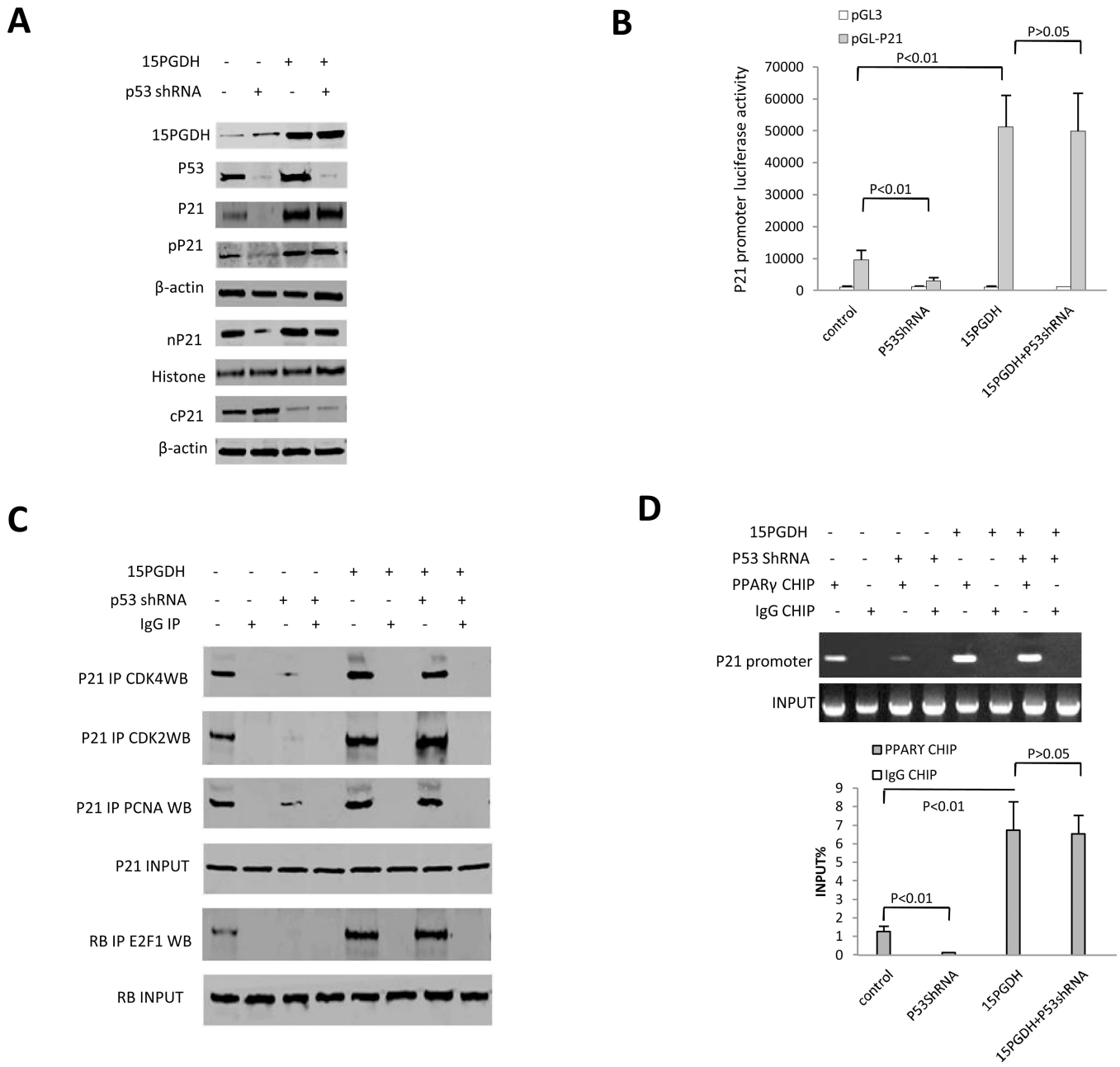

Figure 7. The effect of p53 in 15-PGDH-mediated regulation of p21 in HCC cells

A. Western blotting analysis using indicated antibodies in HepG2 cells transfected with GFP control vector and 15-PGDH expression vector with or without co-transfection of the p53 shRNA vector. The level of p21 in the nuclear fraction (nP21) and cytoplasmic fraction (cP21) were examined. β-actin and histone were used as the internal controls.

B. p21 promoter luciferase activity assay in HepG2 cells transfected with the 15-PGDH expression vector or the control vector with or without co-transfection of the p53 shRNA vector. The data are presented as mean±SEM (**p < 0.01).

C. Co-immunoprecipitation and western blotting analysis in HepG2 cells transfected with the control vector or the 15-PGDH expression vector with or without cotransfection of the p53 shRNA vector. IgG IP was used as the negative control.

D. PPARγ CHIP assay in HepG2 cells transfected with the control vector or the 15-PGDH expression vector with or without cotransfection of the p53 shRNA vector (Addgene). (*Upper panel*) CHIP-regular PCR assay. p21 promoter PCR product was used as input. (*Lower panel*) CHIP-real time PCR assay. IgG CHIP was used as the negative control. The data are presented as mean±SEM (**$p < 0.01$ compared with the corresponding control).

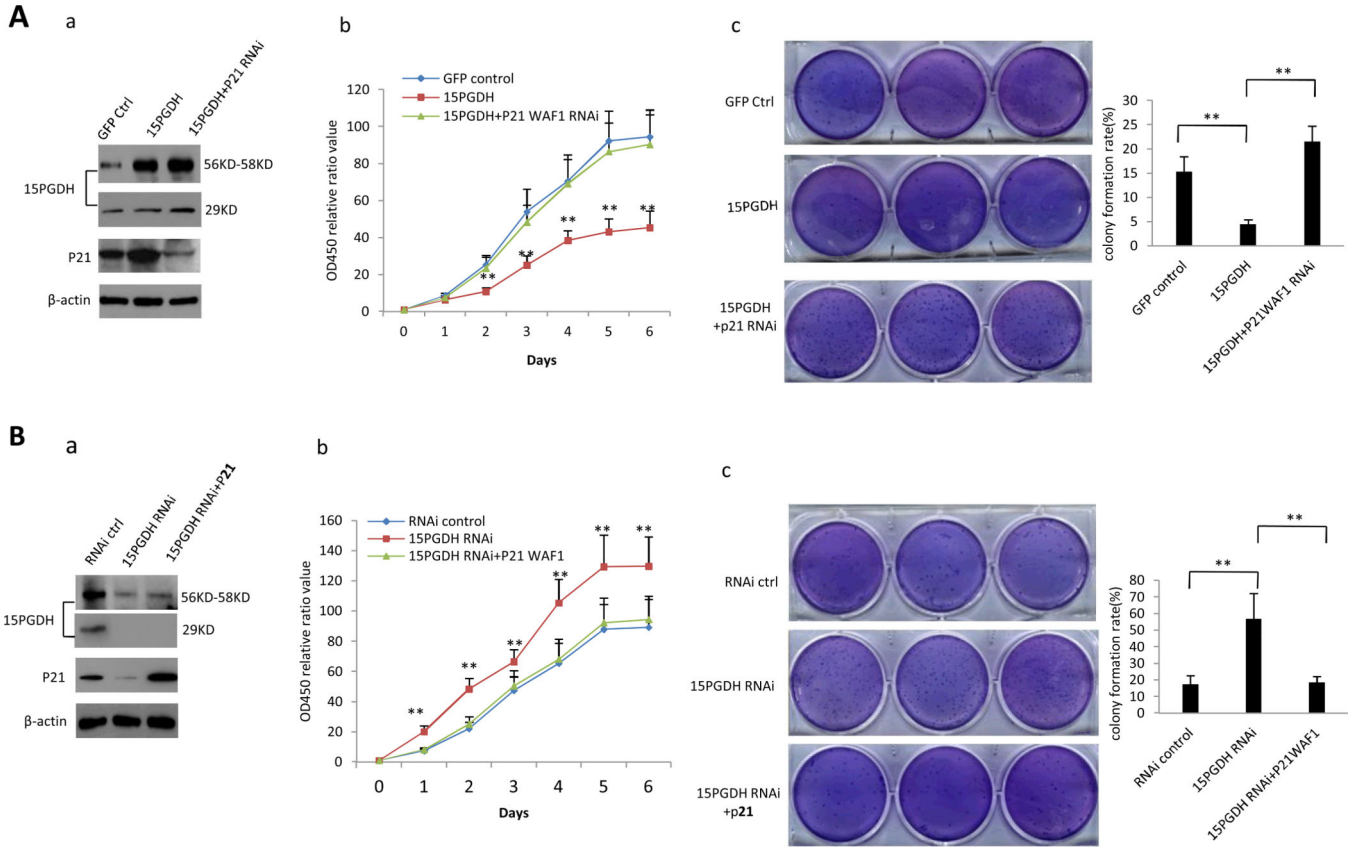

Figure 8. 15-PGDH inhibits HCC cell growth through p21$^{WAF1/Cip1}$

A. Huh7 cells transfected with 15-PGDH overexpression vector with or without co-transfection of p21 RNAi. *a* Western blotting for 15-PGDH and p21 (β-actin was used as loading control). *b* WST cell proliferation assay. Each sample was assayed in triplicate for 6 consecutive days. Data are means±SEM from three independent experiments (**$p < 0.01$). *c* Soft-agar colony formation assay. The results are representative of three independent experiments (**$p < 0.01$).

B. Huh7 stable cell transfected with 15-PGDH RNAi vector with or without co-transfection of p21 expression vector. *a* Western blotting for 15-PGDH and p21 (β-actin was used as loading control). *b* WST cell proliferation assay. Each sample was assayed in triplicate for 6 days consecutively. Data are mean±SEM from three independent experiments (**$p < 0.01$). *c* Soft-agar colony formation assay. The results are representative of three independent experiments (**$p < 0.01$).

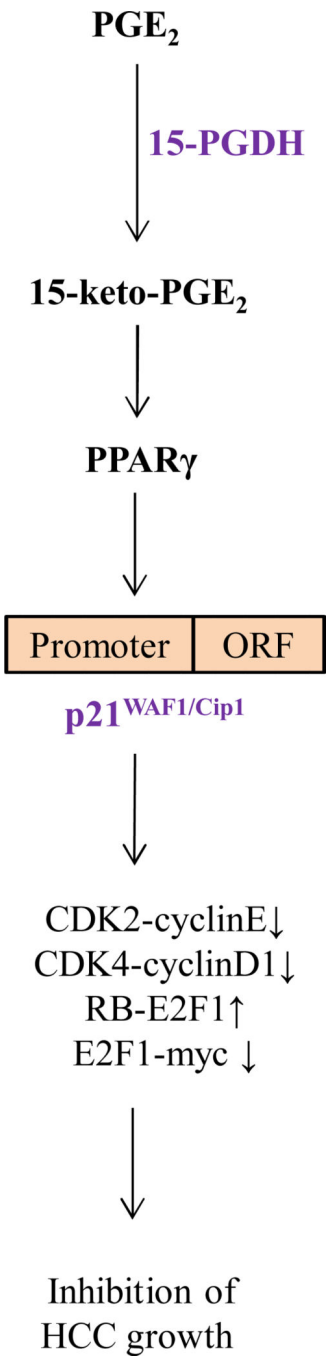

Figure 9.
Schematic illustration of key mechanisms for 15-PGDH-mediated inhibition of hepatocellular carcinoma growth.